

Thick-Plate Model for Warping Stresses in Concrete Pavements

X.P. SHI^a, T.F. FWA^{b*}, Y. HU^c and J. ZHANG^d

^aSS Pavement Consultant 446 Serangoon Road Singapore 218137, ^bDepartment of Civil Engineering National University of Singapore 10 Kent Ridge Crescent Singapore 119260, ^cformerly Research Scholar Department of Civil Engineering National University of Singapore 10 Kent Ridge Crescent Singapore 119260 and ^dResearch Scholar Department of Civil Engineering National University of Singapore 10 Kent Ridge Crescent Singapore 119260

In this paper, a new analytical solution is derived for calculating the warping stresses in concrete pavement slab. In the analysis, we consider the pavement slab as a rectangular thick plate resting on Pasternak foundation. The effects of transverse shear deformation and the interlocking action of subgrade are considered in calculating the warping stresses in concrete pavement slabs. The solutions to the fundamental equations of the problem are obtained by superposing the solutions of two elemental slabs. Each of these elemental slabs has two guided support edges and two free edges each acted upon by an unknown bending moment. Numerical examples are presented to compare the solutions of the proposed model with finite element solutions and the Bradbury-Westergaard solutions. The results suggest that for common highway slab dimensions and thickness, the thick-plate model should be used to estimate thermal warping stresses in pavement slabs with a slab width of 3.5 m. However, the conventional thin-plate model could be used for slabs with a width of 7.0 m or more without incurring significant errors.

Keywords: Concrete pavement, thick-plate model, Pasternak foundation, warping Stress, superposition method

INTRODUCTION

It is well recognised today that the combined effects of load-induced stresses and thermal warping stresses are responsible for causing cracking in concrete pavements. The magnitude of warping stresses due to thermal gradient can be of the same order as that of load-induced stresses. The effect of warping stresses is a major consideration in any mechanistic pavement design procedure.

Westergaard (1927) was the first to present an analytical thin-plate model for the analysis of thermal warping stresses in a concrete pavement slab with infinite width and length. Based on the concepts of Westergaard, Bradbury (1938) developed an approximate solution for concrete pavement slabs with finite dimensions. To consider the geometric configuration of concrete pavements exactly, several numerical models (Chou 1981, Huang 1985, 1993) have been developed by researchers. These analytical and numerical models were developed using thin-plate

* Please direct all correspondence to T.F. Fwa Dept. of Civil Engineering National University of Singapore 10 Kent Ridge Crescent SINGAPORE 119260 Fax: 65-779-1635 e-mail: cvewatf@nus.edu.sg

theory and subgrade models represented by either Winkler foundation or elastic solid foundation. The effects of transverse shear deformation of slab and the interlocking action of subgrade were not considered.

An analytical solution which uses thick-plate theory and Pasternak foundation model (Pasternak 1954) to analyse the behaviour of pavement slabs subjected traffic loading was developed by Shi *et al.* (1994), and was compared with the widely used Bradbury-Westergaard solution and solutions by several numerical methods on the same subject. The comparisons clearly show that transverse shear deformation and interlocking action of subgrade have significant effects on the computed stresses in concrete pavements under traffic loads.

Shi *et al.* (1993) have developed an analytical thin-plate model for the analysis of warping stresses in concrete pavements resting on Pasternak foundation. It was found that pavement models with Winkler foundation overestimate warping stresses. Shi *et al.* (1993) concluded that, depending on the slab dimensions, slab and subgrade properties, the Winkler foundation model of Bradbury-Westergaard could lead to overestimation of warping stress by as much as 17%. The model by Shi *et al.* (1993) was derived

using thin-plate theory without considering the influence of transverse shear deformation in the slab. Furthermore, it employed the approximate method of Bradbury (1938) to represent the finite slab conditions.

In the present paper, a thick-plate model for the analysis of thermal warping stresses in a concrete pavement slab with four free edges resting on a Pasternak foundation is developed. The effects of transverse shear deformation and interlocking action of subgrade are considered. Fundamental equations for this pavement model are developed based on the Reissner thick-plate theory (Reissner 1945) and the Pasternak foundation model. The analysis considers only linear thermal gradient through the slab's thickness, and excludes the effects of the self-weight of pavement slab. The solution to the fundamental equations is obtained by superposing the solutions of two elemental slabs as shown in Figure 1. The solutions by the proposed model are compared with those by the conventional numerical and analytical methods, as well as some measurements of full-size experimental slabs.

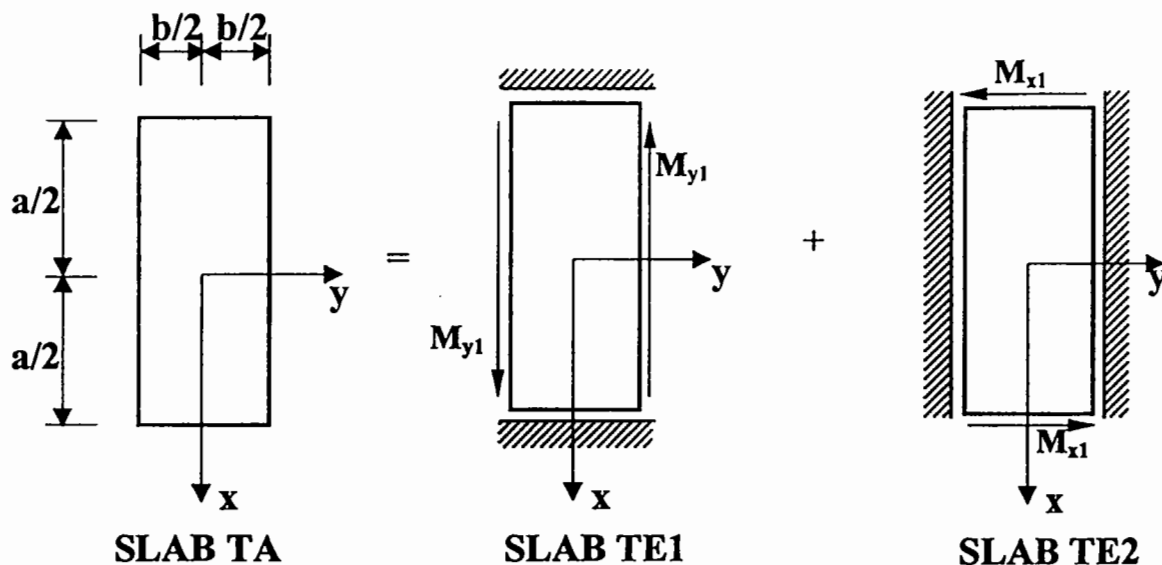


FIGURE 1 Superposition of Elemental Slabs

FUNDAMENTAL EQUATIONS

The derivation presented in this paper is based on the following assumptions:

- (1) Concrete pavement slabs are assumed to be thick plates that are elastic, homogeneous, and isotropic with temperature-independent material properties;
- (2) The subgrade is assumed to be a Pasternak foundation, with Winkler foundation as one of its special cases;
- (3) Plane sections remain plane after deformation;
- (4) There is no friction between pavement and subgrade;
- (5) Slab temperature varies linearly through its thickness;
- (6) The deflection of the slab is small compared with the slab dimensions; and
- (7) The coordinate system is such that z is considered positive upward and measured from mid-plane of the plate

Considering the strains induced by variations of temperature, by setting the vertical load $q = 0$, the fundamental equations for a thick plate with a linear temperature gradient across its thickness can be obtained in a similar form to those for bending problems (Shi et al. 1994):

$$\nabla^4 w - \frac{c^2 k + G_b}{D_1} \nabla^2 w + \frac{k}{D_1} w = 0 \quad (1a)$$

$$\frac{h^2}{10} \nabla^2 Q_x - Q_x = D_2 \frac{\partial}{\partial x} (\nabla^2 w) - \frac{kh^2}{10(1-\mu)} \frac{\partial w}{\partial x} \quad (1b)$$

$$\frac{h^2}{10} \nabla^2 Q_y - Q_y = D_2 \frac{\partial}{\partial y} (\nabla^2 w) - \frac{kh^2}{10(1-\mu)} \frac{\partial w}{\partial y} \quad (1c)$$

$$M_x = D \left[\frac{6(1-\mu)}{5Gh} \frac{\partial V_x}{\partial x} - \left(G_1 \frac{\partial^2 w}{\partial x^2} + G_2 \frac{\partial^2 w}{\partial y^2} \right) + \frac{3\mu kw}{5Gh} \right] + M_T \quad (1d)$$

$$M_y = D \left[\frac{6(1-\mu)}{5Gh} \frac{\partial V_y}{\partial y} - \left(G_1 \frac{\partial^2 w}{\partial y^2} + G_2 \frac{\partial^2 w}{\partial x^2} \right) + \frac{3\mu kw}{5Gh} \right] + M_T \quad (1e)$$

$$M_{xy} = \frac{Gh^3}{12} \left[\frac{6}{5Gh} \left(\frac{\partial V_x}{\partial y} + \frac{\partial V_y}{\partial x} \right) - 2 \frac{\partial^2 w}{\partial x \partial y} \right] \quad (1f)$$

$$p = -kw + G_b \nabla^2 w \quad (1g)$$

$$\alpha = \frac{6}{5Gh} V_x - \frac{\partial w}{\partial x} \quad (1h)$$

$$\beta = \frac{6}{5Gh} V_y - \frac{\partial w}{\partial y} \quad (1i)$$

where h , E , μ , G_b , k , α_t and Δ_t are respectively the slab thickness, the slab modulus, the Poisson's ratio of the slab, the shear modulus of the foundation, the subgrade reaction modulus, the coefficient of thermal expansion of concrete, and temperature difference between the top and bottom of the slab respectively. Displacements, u , v , and w_z are positive when they act in the positive directions of the x -, y - and z -axis, respectively. They are assumed to be of the form $u = z\alpha(x, y)$, $v = z\beta(x, y)$ and w_z given by $w(x, y)$, which is constant over the slab thickness; where α and β are the rotations in the xz - and yz -planes, respectively, of a line element originally perpendicular to the neutral surface, and w is the vertical displacement of all points on this line element.

Other parameters in the equations are given by

$$D = [Eh^3/(1-\mu^2)]/12;$$

$$G = [E/(1-\mu)]/2; \quad (1j)$$

$$D_1 = D + c^2 G_b;$$

$$D_2 = [D + G_b h^2/(1-\mu)]/10; \quad (1k)$$

$$G_1 = 1 + [(3\mu G_b/G)/h]/5;$$

$$G_2 = \mu + [(3\mu G_b/G)/h]/5. \quad (1l)$$

$$M_T = (1+\mu)D\alpha_t\Delta_t/h;$$

$$c^2 = [h^2(2-\mu)/(1-\mu)]/10; \quad (1m)$$

Eqs. (1a)-(1m) are the fundamental equations for solving the problem concerning the thermal warping of a thick plate resting on the Pasternak foundation.

The general solution of w , Q_x and Q_y are obtained through solving the governing equations (1a), (1b) and (1c). Other resultants of the plate are then determined from Eqs. (1d) to (1I) by substituting the general solutions of w , Q_x , and Q_y into these equations.

However, only in a few simple cases, the general solutions of w , Q_x and Q_y can be directly obtained from the governing Eqs. (1a), (1b) and (1c). In most cases, the governing equations have to be converted to another form. By writing the general solutions for w , Q_x and Q_y as the sum of a complementary and particular function, respectively,

$$\begin{aligned} w &= w_c + w_p & Q_x &= Q_{xc} + Q_{xp} \\ & & Q_y &= Q_{yc} + Q_{yp} \end{aligned} \quad (1n)$$

and introduce a function $\psi(x, y)$ so that

$$Q_{xc} = \frac{\partial \psi}{\partial y} \quad Q_{yc} = \frac{\partial \psi}{\partial x} \quad (1o)$$

the governing equations can be rewritten as follows:

$$\nabla^4 w_c - \frac{c^2 k + G_b}{D_1} \nabla^2 w_c + \frac{k}{D_1} w_c = 0 \quad (1p)$$

$$\nabla^4 w_p - \frac{c^2 k + G_b}{D_1} \nabla^2 w_p + \frac{k}{D_1} w_p = 0 \quad (1q)$$

$$\frac{h^2}{10} \nabla^2 \psi - \psi = 0 \quad (1r)$$

$$Q_{xp} = Q_x^* + \frac{\partial}{\partial x} (-D_1 \nabla^2 w_c + c^2 k w) \quad (1s)$$

$$Q_{yp} = Q_y^* + \frac{\partial}{\partial y} (-D_1 \nabla^2 w_c + c^2 k w) \quad (1t)$$

in which Q_x^* and Q_y^* are functions that must satisfy the following equations:

$$\frac{h^2}{10} \nabla^2 Q_x^* - Q_x^* = D_2 \frac{\partial}{\partial x} (\nabla^2 w_p) - \frac{kh^2}{10(1-\mu)} \frac{\partial w_p}{\partial x} \quad (1u)$$

$$\frac{h^2}{10} \nabla^2 Q_y^* - Q_y^* = D_2 \frac{\partial}{\partial y} (\nabla^2 w_p) - \frac{kh^2}{10(1-\mu)} \frac{\partial w_p}{\partial y} \quad (1v)$$

SOLUTION OF ELEMENTAL SLABS TE1 AND TE2

The boundary conditions of the elemental slab TE1 (see Figure 1) with two guided support edges and two free edges each acted upon by an unknown moment are:

$$V_x \left(\pm \frac{a}{2}, y \right) = M_{xy} \left(\pm \frac{a}{2}, y \right) = \alpha \left(\pm \frac{a}{2}, y \right) = 0 \quad (2a)$$

$$V_y \left(x, \pm \frac{b}{2} \right) = M_{xy} \left(x, \pm \frac{b}{2} \right) = 0 \quad (2b)$$

$$M_y \left(x, \pm \frac{b}{2} \right) = M_{y1} \quad (2c)$$

the complementary functions can be assumed to take the following forms:

$$w_c = \sum_{m=0}^{\infty} Y_m(y') \cos \left(\frac{m\pi}{a} x' \right) \quad (3a)$$

$$\psi = \sum_{m=0}^{\infty} Z_m(y') \sin \left(\frac{m\pi}{a} x' \right) \quad (3b)$$

Making use of the symmetry of temperature gradient about x- and y-axis, the boundary conditions of the guided support edges Equation (2a) can be satisfied with the following expressions:

$$w_c = \quad (3c)$$

$$\sum_{m=0}^{\infty} [A_m cc(y) + D_m ss(y)] (-1)^{m/2} \cos \left(\frac{m\pi}{a} x \right)$$

$$\psi = \sum_{m=0}^{\infty} H_m \sinh(\beta_m y) (-1)^{m/2} \sin \left(\frac{m\pi}{a} x \right) \quad (3d)$$

where

$$cc(y) = \cosh(e_m y) \cos(f_m y) \quad (3e)$$

$$ss(y) = \sinh(e_m y) \sin(f_m y) \quad (3f)$$

Furthermore, it is assumed that the unknown bending moment M_{y1} can be represented by Fourier series:

$$M_{y1} = M_T/2 + \sum_{m=0,2}^{\infty} E_m (-1)^{m/2} \cos \left(\frac{m\pi}{a} x \right) \quad (4a)$$

The three intergration constants A_m , D_m and H_m in Eqs. (3c) and (3d) can be expressed by one unknown coefficient E_m based on the boundary conditions of the free edges Equations (2a) to (2c). The solutions of elemental slab TE1 are obtained as follows:

$$w = \sum_{m=0,2}^{\infty} \frac{E_m}{D_1 \Delta_m} [\Delta_{m1} cc(y) + \Delta_{m2} ss(y)] (-1)^{m/2} \cos\left(\frac{m\pi}{a} x\right) \quad (5a)$$

$$\begin{aligned} M_x = M_T/2 & \\ & + \sum_{m=0,2}^{\infty} \frac{E_m}{\Delta_m} [(I_{m5} \Delta_{m1} + I_{m6} \Delta_{m2}) cc(y) \\ & + (I_{m5} \Delta_{m2} - I_{m6} \Delta_{m1}) ss(y) \\ & + I_{m7} \Delta_{m3} \cosh(\beta_m y)] (-1)^{m/2} \cos\left(\frac{m\pi}{a} x\right) \end{aligned} \quad (5b)$$

$$\begin{aligned} M_y = M_T/2 & \\ & + \sum_{m=0,2}^{\infty} \frac{E_m}{\Delta_m} [(I_{m8} \Delta_{m1} - I_{m9} \Delta_{m2}) cc(y) \\ & + (I_{m8} \Delta_{m2} + I_{m9} \Delta_{m1}) ss(y) \\ & - I_{m7} \Delta_{m3} \cosh(\beta_m y)] (-1)^{m/2} \cos\left(\frac{m\pi}{a} x\right) \end{aligned} \quad (5c)$$

By repeating this process, the solution with unknown coefficient F_n for the elemental slab TE2 can be obtained in similar forms to Equations (5a)-(5c).

DETERMINATION OF UNKNOWN COEFFICIENTS

After superposing the solutions of the two elemental slabs, TE1 and TE2, the resulting solutions of slab TA (see Figure 1) satisfy all the free-edge boundary conditions except the following two:

$$\begin{aligned} \left[M_x \left(\frac{a}{2}, y \right) \right]_{TA} &= \left[M_x \left(\frac{a}{2}, y \right) \right]_{TE1} \\ &+ \left[M_x \left(\frac{a}{2}, y \right) \right]_{TE2} = 0 \end{aligned} \quad (6a)$$

$$\begin{aligned} \left[M_y \left(x, \frac{b}{2} \right) \right]_{TA} &= \left[M_y \left(x, \frac{b}{2} \right) \right]_{TE1} \\ &+ \left[M_y \left(x, \frac{b}{2} \right) \right]_{TE2} = 0 \end{aligned} \quad (6b)$$

After substituting Equations (5b) and (5c) into Equation (6) and applying Fourier transform, we can obtain the following linear equations to determine the two unknown coefficients E_m and F_n :

$$\begin{aligned} \sum_{n=0,2}^{\infty} \sum_{m=0,2}^{\infty} (-1)^{n/2} T_{mn} E_m \cos\left(\frac{n\pi}{b} y\right) \\ + \sum_{n=0,2}^{\infty} (-1)^{n/2} F_n \cos\left(\frac{n\pi}{b} y\right) + M_T = 0 \end{aligned} \quad (7a)$$

$$\begin{aligned} \sum_{m=0,2}^{\infty} \sum_{n=0,2}^{\infty} (-1)^{m/2} U_{mn} F_n \cos\left(\frac{m\pi}{a} x\right) \\ + \sum_{m=0,2}^{\infty} (-1)^{m/2} E_m \cos\left(\frac{m\pi}{a} x\right) + M_T = 0 \end{aligned} \quad (7b)$$

where

$$\begin{aligned} T_{mn} = \frac{2\lambda}{b} \int_{-b/2}^{b/2} \left\{ \frac{1}{\Delta_m} [(I_{m5} \Delta_{m1} + I_{m6} \Delta_{m2}) cc(y) \right. \\ \left. + (I_{m5} \Delta_{m2} - I_{m6} \Delta_{m1}) ss(y) \right. \\ \left. + I_{m7} \Delta_{m3} \cosh(\beta_m y)] \right\} \cos\left(\frac{n\pi}{b} y\right) dy \end{aligned} \quad (7c)$$

$$\begin{aligned} U_{mn} = \frac{2\lambda}{b} \int_{-a/2}^{a/2} \left\{ \frac{1}{\Delta_m} [(I_{n5} \Delta_{n11} + I_{n6} \Delta_{n12}) cc(x) \right. \\ \left. + (I_{n5} \Delta_{n12} - I_{n6} \Delta_{n11}) ss(x) \right. \\ \left. + I_{n7} \Delta_{n13} \cosh(\beta_n x)] \right\} \cos\left(\frac{m\pi}{a} x\right) dx \end{aligned} \quad (7d)$$

Δ_{mi} , I_{mi} , and I_{ni} in Eqs. (5a) to (5c), (7c) and (7d) can be determined by the formula developed in an earlier work (Shi et al. 1994).

SOLUTION FOR SLAB TA

Since M_T in Equation (7) is a constant, E_m and F_n have to be zero when m or $n > 0$. Thus E_0 and F_0 can be easily obtained. After substituting them into Equation (5a) to (5c), we can obtain the solutions of the ele-

mental slabs and then the solution for slab TA by the method of superposition. The solutions for SLAB TE1 and TE2 can be determined as follows:

$$(w)_{TE1} = \frac{U_{00} - 1}{1 - U_{00}T_{00}} \\ 2M_T \left\{ \frac{1}{D_1 \Delta_m} [\Delta_{m1} cc(y) + \Delta_{m2} ss(y)] \right\}_{m=0} \quad (8a)$$

$$(M_x)_{TE1} = \frac{U_{00} - 1}{1 - U_{00}T_{00}} 2M_T \left\{ \frac{1}{\Delta_m} [(I_{m5} \Delta_{m1} + I_{m6} \Delta_{m2}) cc(y) + (I_{m5} \Delta_{m2} - I_{m6} \Delta_{m1}) ss(y)] \right\}_{m=0} + M_T \quad (8b)$$

$$(M_y)_{TE1} = \frac{U_{00} - 1}{1 - U_{00}T_{00}} 2M_T \left\{ \frac{1}{\Delta_m} [(I_{m8} \Delta_{m1} - I_{m9} \Delta_{m2}) cc(y) + (I_{m8} \Delta_{m2} + I_{m9} \Delta_{m1}) ss(y)] \right\}_{m=0} + M_T \quad (8c)$$

and

$$(w)_{TE2} = \frac{T_{00} - 1}{1 - U_{00}T_{00}} \\ 2M_T \left\{ \frac{1}{D_1 \Delta_n} [\Delta_{n11} cc(x) + \Delta_{n12} ss(x)] \right\}_{n=0} \quad (8d)$$

$$(M_y)_{TE2} = \frac{T_{00} - 1}{1 - U_{00}T_{00}} 2M_T \left\{ \frac{1}{\Delta_n} [(I_{n5} \Delta_{n11} + I_{n6} \Delta_{n12}) cc(x) + (I_{n5} \Delta_{n12} - I_{n6} \Delta_{n11}) ss(x)] \right\}_{n=0} + M_T \quad (8e)$$

$$(M_x)_{TE2} = \frac{T_{00} - 1}{1 - U_{00}T_{00}} 2M_T \left\{ \frac{1}{\Delta_n} [(I_{n8} \Delta_{n11} - I_{n9} \Delta_{n12}) cc(x) + (I_{n8} \Delta_{n12} + I_{n9} \Delta_{n11}) ss(x)] \right\}_{n=0} + M_T \quad (8f)$$

Thermal warping stresses σ_x and σ_y in the slab TA can be determined as follows:

$$\sigma_x = \frac{6[(M_x)_{TE1} + (M_x)_{TE2}]}{h^2} \quad (9a)$$

$$\sigma_y = \frac{6[(M_y)_{TE1} + (M_y)_{TE2}]}{h^2} \quad (9b)$$

VERIFICATION USING NUMERICAL EXAMPLES

Comparison with Finite Element Solutions

Verification of the proposed approach is made against an established finite element model KENSLABS. KENSLABS is a finite element program developed by Huang (1985) for the structural analysis of rigid pavement slab supported on either Winkler foundation or solid foundation. The formulation of KENSLAB is based on thin-plate theory. Results obtained by the proposed model are compared with those by KENSLABS for different thicknesses of a single pavement slab resting on a Winkler foundation. Winkler foundation is analyzed by setting the shear modulus of subgrade, G_b , to zero in the proposed model developed in this paper. The slabs are assumed to be in full contact with the subgrade. To eliminate the influences of slab sizes and transverse shear deformation in the slab, a large and thin square slab is used in the comparison. The slab is 10.2 m (400 in.) long with a Young's modulus of 34.5 GPa (5×10^6 psi), a Poisson ratio of 0.2, a coefficient of thermal expansion of $9 \times 10^{-6}/^\circ\text{C}$ ($5 \times 10^{-6}/^\circ\text{F}$), and a temperature differential of 0.066 $^\circ\text{C}$ per mm (3°F per in.) of the slab. Four different moduli of subgrade reaction of 13.6, 27.1, 54.3 and 135.7 MN/m^3 (50, 100, 200 and 500 pci) and four different slab thicknesses of 152, 203, 254 and 305 mm (6, 8, 10 and 12 in.) are considered. There are altogether a total of 16 cases. Table I shows the maximum interior warping stresses obtained by the proposed model and KENSLABS. The agreement between the two solutions is excellent for all the 16 cases.

Comparison with Full-Size Slab Experiment and theoretical solutions

Full-size slab experiments of thermal warping were carried out by Yao and Huan (1984) on a group of 20-cm-thick concrete slabs with a uniform width of 4.5 m and three lengths of 4.5 m, 5.5 m and 6.5 m, respectively. These test slabs were constructed on a section of old asphalt pavement road in Hefei, China. A 24-cm-thick subbase treated with 10% lime was

used to provide a uniform support for the slabs. Warping strains were measured by preinstalled 4-cm strain gauges as well as portable strain meters. The average modulus of subgrade reaction measured in the experiment site on the surface of the subbase was 80 MN/m³. The average elasticity modulus of concrete was measured to be equal to 30,000 MPa. The Poisson's ratio of the slab was 0.15.

The shear modulus of the subgrade G_b was determined by a method developed by Fwa et al. (1996) that estimates G_b as a function of the modulus of subgrade reaction k . Readers are referred to the paper by Fwa et al. (1996) for the detailed derivation of the relationship between G_b and k . In the analysis of the experiment results by Yao and Huan, G_b can be calculated to be 28 MN/m from the measured value of k . The reported stresses of the experiment slabs were calculated based on the measured strain values.

Table II provides a comparison of the accuracy of predictions by the proposed and other solutions. The comparison is made in terms of a dimensionless warping stress coefficient, computed by dividing the maximum interior warping stress by $(E \cdot \alpha_t \cdot \Delta T)$. Table II shows that the Bradbury-Westergaard solutions produce warping stresses 15–19% higher than the experimental results, while KENSLABS solutions yield 14–20% errors. The errors are due to non-consideration of the effects of transverse shear deforma-

tion of slab and the shear modulus of subgrade. By incorporating the effect of transverse shear deformation of slab through the adoption of the proposed thick-plate model, better results were obtained, especially for the smaller slab sizes. The errors of the proposed solutions with Winkler foundation model are about 12%. The improvements resulting from employing the proposed thick-plate model and Pasternak foundation are apparent from this comparison. The maximum error is 5.5%.

Thin-Plate versus Thick-Plate Models

This section provides further comparisons between thin-plate and thick-plate models. Two rectangular slabs resting on Winkler foundation with the respective widths of 3.5 m (138 in.) and 7 m (276 in.) are analysed by the proposed thick-plate model and the thin-plate finite element model KENSLABS (Huang 1993). The parameters of the problem are: $E = 20,000$ MPa (2.9×10^6 psi), $\mu = 0.15$, $k = 200$ MN/m³ (368.6 pci), $\Delta T/h = 80^\circ\text{C}/\text{m}$ ($3.7^\circ\text{F}/\text{in.}$), $\alpha_t = 9 \times 10^{-6}/^\circ\text{C}$ ($5 \times 10^{-6}/^\circ\text{F}$). The maximum interior warping stress, the maximum edge warping stress along the length of the slab, and the maximum warping stress along the width of the slab determined by these two models are compared.

TABLE I Comparison of maximum interior warping stresses in large thin slabs

Slab thickness (mm)	Method	Maximum interior warping stress (MPa)			
		$k=13.6$ MN/m ³	$k=27.1$ MN/m ³	$k=54.3$ MN/m ³	$k=135.7$ MN/m ³
152	KENSLABS	2.076	1.991	1.941	1.934
	Proposed	2.080	2.000	1.949	1.940
203	KENSLABS	2.843	2.793	2.681	2.585
	Proposed	2.850	2.803	2.695	2.601
254	KENSLABS	3.427	3.554	3.487	3.306
	Proposed	3.439	3.564	3.502	3.330
305	KENSLABS	3.774	4.169	4.264	4.095
	Proposed	3.790	4.180	4.276	4.120

Note: Interior warping stresses of large thin slabs are considered to minimize the effect of thick plate. Winkler foundation is assumed for both KENSLABS and the proposed model.

TABLE II Coefficient of maximum interior warping stress

Slab Size (m)	4.5 by 4.5	5.5 by 4.5	6.5 by 4.5
Experimental results	0.479	0.536	0.546
Bradbury-Westergaard solution ^a	0.570	0.622	0.629
Error (%)	+19.0%	+16.1%	+15.2%
KENSLABS solution ^b	0.577	0.627	0.626
Error (%)	+20.5%	+17.0%	+14.7%
Proposed Winkler solution ^c	0.533	0.597	0.614
Error (%)	+11.3%	+11.4%	+12.5%
Proposed Pasternak solution ^d	0.475	0.546	0.576
Error (%)	-0.8%	+1.9%	+5.5%

- a. Bradbury-Westergaard solution with Winkler foundation model (Bradbury 1938).
b. Finite element solution based on thin-plate and Winkler foundation model (Huang 1993)
c. Proposed thick-plate solution with Winkler foundation model.
d. Proposed thick-plate solution with Pasternak foundation model.

The comparison of the computed maximum interior warping stresses of the slabs are shown in Figure 2. Figure 3 and Figure 4 plot the results of the computed maximum edge warping stresses along the length and the width of slab, respectively. The errors in warping stresses computed by the thin-plate model are listed in Table III. The following observations can be made: (1) Of the three warping stresses computed by the thin-plate model, the interior warping stress has the smallest errors. The largest errors are associated with computed edge warping stresses along the width of the slabs. (2) The maximum warping stresses determined by the thin-plate model are very close to those determined by the thick-plate model when the slab is thin, say 200 mm or less. (3) Errors of the thin-plate model increase as the thickness of slab increases. (4) Errors of the thin-plate model decrease with an increase of slab length for the case of interior warping stresses, and the case of edge warping stresses along the length of slab. However, the situation is reverse for the edge warping stresses along the width of slab. (5) As indicated by the results in Table III, errors in all warping stresses decrease when the slab width (the smaller of the plane dimensions of the slab) is increased.

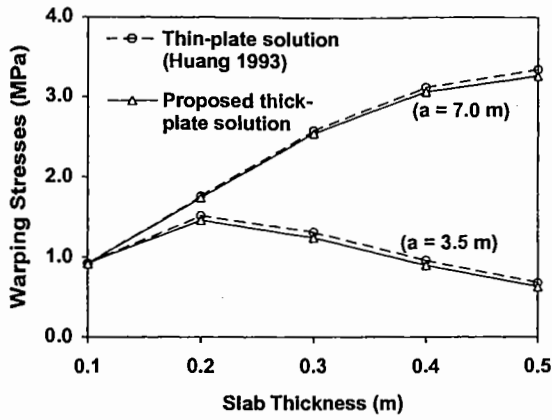
The analysis results suggest that thin-plate models can be used for estimating the interior warping stress.

For a slab with a width of 3.5 m or more, the errors in the interior warping stress computed by a thin-plate model are found to be less than 10%. They are less than 5% when the slab thickness is 200 mm or less. The errors in the computed edge warping stresses are higher, especially along the shorter edge of the slabs. Errors can be as much as 31.6% when the slab width is 3.5 m, which is a common slab width for concrete highway pavements.

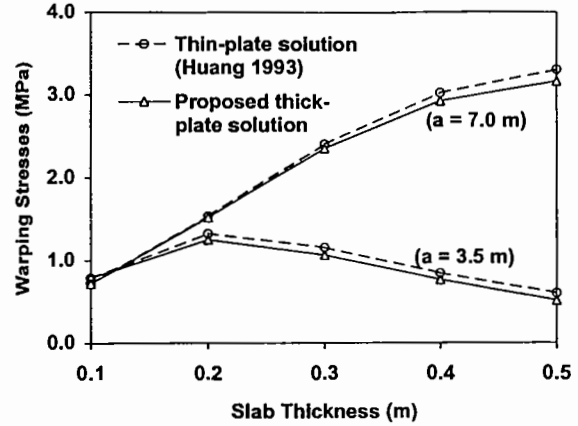
It can be seen from Table III that the magnitude of errors involved with the use of thin-plate model decrease significantly when the slab width is increased to 7.0 m. For the common range of highway pavement slab dimensions and thickness, the errors are likely to be less than 5% for the interior and edge warping stresses computed by the thin-plate model.

SUMMARY

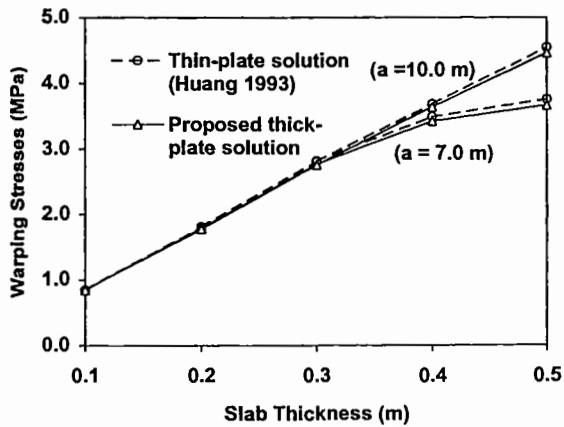
A thick-plate model for computing thermal warping stress in concrete pavements has been developed using the Reissner thick-plate theory and the Pasternak foundation model. This proposed model considers the effects of interlocking action of subgrade and transverse shear deformation of slab. The thick-plate solutions derived in this paper were validated by com-



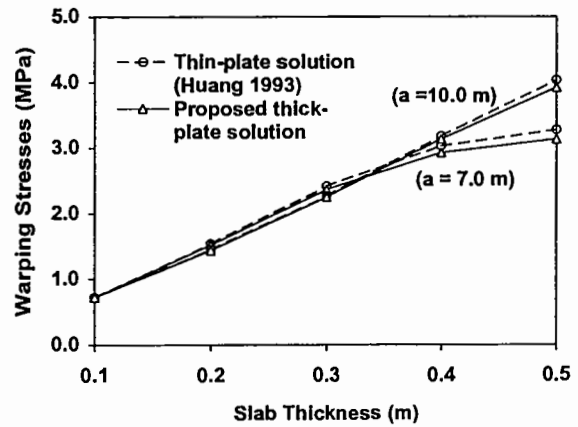
(i) Width of Slab $b = 3.5$ m



(i) Width of Slab $b = 3.5$ m



(ii) Width of Slab $b = 7.0$ m



(ii) Width of Slab $b = 7.0$ m

FIGURE 2 Comparison of Maximum Interior Warping Stresses of a Rectangular Slab Supported on Winkler foundation

FIGURE 3 Comparison of Maximum Edge Warping Stresses along Length of a Rectangular Slab Supported on Winkler Foundation

parison with finite element results and experiment data.

Further analyses were conducted to compare the differences in thin-plate and thick-plate solutions for warping stresses. The following conclusions can be drawn from the analyses:

- (1) The use of thin-plate model does not yield significantly errors in the computed interior warping stresses of a slab for the common range of highway pavement slab sizes and thickness. It can be used to estimate interior warping stresses for con-

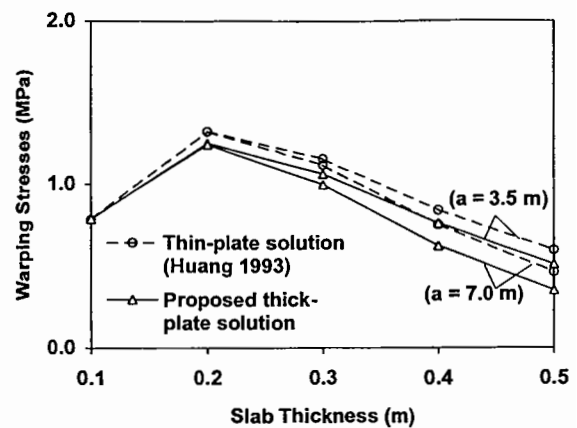
crete pavement slabs. The differences between the thin-plate and thick-plate solutions are less than 5% for slab thickness less than 200 mm. They tend to increase for slabs with thicker thickness. The thin-plate model overestimates interior warping stresses by about 8% for a 3.5 m square slab with a thickness of 500 mm.

- (2) The use of thin-plate model may result in significant errors in the computed edge warping stresses of a slab. For a highway pavement slab with a width of 3.5 m, the thin-plate model pro-

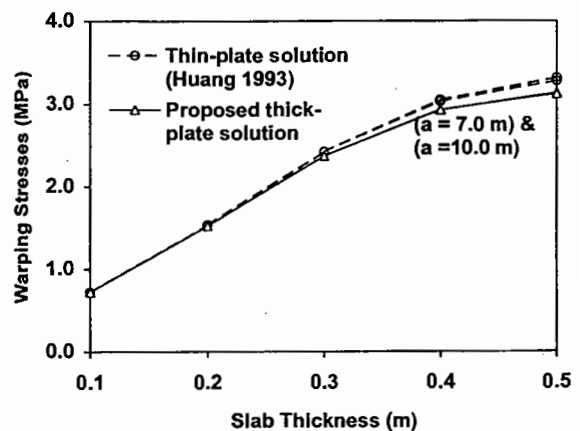
duces 17% and 32% errors in the maximum edge stresses along the length and the width of slab, respectively. For concrete highway slabs with a width of about 3.5 m, it is recommended that the proposed thick-plate model be used for computing thermal warping stresses. When the slab width is 7.0 m or more, the conventional thin-plate model could be used as the errors are likely to be less than 5% for the common slab dimensions and thickness.

NOTATIONS

- a = length of slab;
- b = width of slab;
- E = elasticity modulus of slab;
- G_b = shear modulus of foundation;
- h = thickness of slab;
- k = reaction modulus of foundation;
- M_x, M_y = bending moments in slab;
- M_{xy} = twisting moment in slab;
- q = intensity of load on slab;
- V_x, V_y = shear forces in slab;
- α, β rotation in the xz - and yz -planes, respectively, of a line element originally perpendicular to the neutral surface;
- α_t coefficient of thermal expansion; and
- ΔT difference of temperature between slab top and bottom.



(i) Width of Slab $b = 3.5$ m



(ii) Width of Slab $b = 7.0$ m

FIGURE 4 Comparison of Maximum Edge Warping Stresses along Width of a Rectangular Slab Supported on Winkler Foundation

TABLE III Error of warping stresses computed by thin-plate model

Width of Slab (m)	Length of Slab (m)	Location of Computed Stress	Thickness of Slab (m)				
			0.1	0.2	0.3	0.4	0.5
3.5	3.5	interior	0.0	3.9	5.6	6.7	8.0
		along length	0.1	5.8	8.7	10.5	17.3
		along width	0.1	5.8	8.7	10.5	17.3
	7.0	interior	0.1	1.5	2.0	2.3	2.8
		along length	0.3	1.3	2.6	3.7	4.6
		along width	0.4	6.6	12.8	20.5	31.6

Width of Slab (m)	Length of Slab (m)	Location of Computed Stress	Thickness of Slab (m)				
			0.1	0.2	0.3	0.4	0.5
7.0	7.0	interior	0.1	1.5	1.8	2.0	2.5
		along length	0.1	1.1	2.2	3.5	4.5
		along width	0.1	1.1	2.2	3.5	4.5
	10.0	interior	0.0	1.1	1.5	1.8	2.0
		along length	0.1	1.0	1.2	1.4	2.9
		along width	0.1	1.1	2.2	4.1	6.2

Note: Each value in the table represents error in percent with respect to the corresponding thick-plate solution.

References

- Bradbury, R.D. (1938). *Reinforced concrete pavements*, Wire Reinforcement Institute, Washington, D.C.
- Chou, Y.T. (1981). "Structural analysis computer programs for rigid multicomponent pavement structures with discontinuities -- WESLIQUID and WESLAYER." *Technical rep. GL-81-6*, U.S. Army Engineer Waterways Experiment Station, Reports 1, 2 and 3.
- Fwa, T.F., Shi, X.P. and Tan, S.A. (1996) "Use of Pasternak foundation model in concrete pavement analysis." *J. Transp. Engrg.*, ASCE, 122(4), pp. 323 – 328.
- Huang, Y.H. (1985). "A computer package for structural analysis of concrete pavements." *Proc. 3rd Int. Conf. on Concrete Pavement Design and Rehabilitation*, Purdue University, pp. 295 – 307.
- Huang, Y.H. (1993). *Pavement analysis and design*, 1st Ed., Prentice Hall, Inc., Englewood Cliffs, N.J.
- Pasternak, P.L. (1954). "On a new method of analysis of an elastic foundation by means of two foundation constants." *Gps. Izd. Lit. po. Strait i Arkh.* (in Russian).
- Reissner, E. (1945). "Effect of transverse shear deformation on elastic plates." *J. Appl. Mech.*, 12, pp. 69 – 77.
- Shi, X.P., Fwa, T.F. and Tan, S.A. (1993). "Warping stresses in concrete pavements on Pasternak Foundation." *J. Transp. Engrg.*, ASCE, 119(6), pp. 905–913.
- Shi, X.P., Tan, S.A. and Fwa, T.F. (1994). "Rectangular thick plate with free edges on Pasternak foundation." *J. Engrg. Mech.*, ASCE, 120(5), pp. 971 – 988.
- Westergaard, H.M. (1927). "Analysis of stresses in concrete pavements caused by variation of temperature." *Public Roads*, 8(3), pp. 54–60.
- Yao, Z.K. and Huan, L.Y. (1984). "Experimental analysis of warping stresses in concrete pavements." *J. East China Highway*, 3, pp. 1–7 (in Chinese).